

Transient Electromagnetic-Thermal FE-Model of a SPICE-Coupled Transformer Including Eddy Currents with COMSOL Multiphysics 4.2

H. Neubert^{*1}, T. Bödrich¹, and R. Disselnkötter²

¹Institute of Electromechanical and Electronic Design, Technische Universität Dresden, Germany,

²ABB AG, Forschungszentrum Deutschland, Germany

* Corresponding author: TU Dresden, IFTE, 01026 Dresden, Germany, holger.neubert@tu-dresden.de

Abstract: Operation of a transformer is characterised by strong dynamic interactions between the electrical subsystems on the primary and secondary sides and the magnetic subsystem. Transient finite element (FE) analysis of a transformer together with SPICE-coupled external electrical sources and loads is a powerful tool for the analysis and design of transformers. This paper describes electromagnetic and thermal 3D FE modelling and transient simulation of a current transformer with focus on the non-linear characteristic of the ferromagnetic transformer core, the coupling of the transformer windings to external circuitry, and the effects of eddy currents and self-heating.

Keywords: transformer, transient analysis, 3D finite element model, SPICE, non-linear ferromagnetic material

1. Introduction

Current transformers are used to measure high currents in power grid systems. Normally, the primary winding consists of only one turn (the power line), whereas the secondary winding is made up of multiple turns (normally some hundreds up to thousands). The secondary winding is operated close to short-circuit condition in order to realize low overall transformer impedance and to avoid high voltages at the secondary side [1]. This short-circuit operation leads together with a highly permeable core material to small flux densities within the transformer core and hence to small ferromagnetic hysteresis losses and measurement errors.

Transient finite element (FE) analysis is a powerful means to design the interactions between external electrical sources and loads respectively and the magnetic subsystem of such a transformer. It also allows to consider self-heating and the temperature-dependent material properties.

A first realisation of a transient 3D FE transformer model using COMSOL Multiphysics 3.5a

was presented in [2]. In the paper presented now, substantial model advances, most notably in the implementation of non-linear magnetic materials, the consideration of eddy currents and the incorporation of a thermal model, will be discussed.

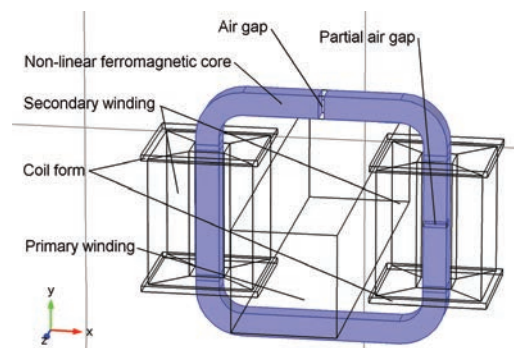


Figure 1. Geometry of the 3D transformer model

Figure 1 shows the principle structure of an investigated current transformer by means of its 3D FE model. As a peculiarity of this device, the ferromagnetic core contains a partial air gap at the right and a full air gap at the top core section. Especially the latter air gap causes an imperfect coupling between the primary and the secondary winding in this particular case. Furthermore, the air gaps within the core lead to an asymmetric model geometry. Hence, a complete 3D model is necessary.

The geometry is generated parametrically. This allows for efficient analysis and design optimization later on. Unlike in the previous study [2], the coil bobbins are also modelled, because they have an influence on the thermal behavior.

2. Electromagnetic Model of the Transformer

The electromagnetic FE model computes the interactions between the electrical subsystem on the primary and secondary sides and the magnetic subsystem. They are described by Ampère's circuital law and Faraday's law of induction. Due

to the non-linear behavior of the ferromagnetic core, the problem cannot be solved in the frequency domain but requires a time-dependent simulation instead. We used the *mf* mode in COMSOL Multiphysics 4.2 because only this mode allows a time-dependent analysis. However, it only solves for the magnetic vector potential \mathbf{A} . This must be taken into account in the loss calculation. The *mfe* mode which solves also for the electric field is not suitable for time-dependent analysis.

The sinusoidal primary current $i_1(t)$ in the power line is modeled as a total current density $J_z(\mathbf{r},t)$ in axial direction of the primary bus bar. However, $J_z(\mathbf{r},t)$ can not be imposed directly as an external current density, but must be calculated under consideration of the induced eddy currents $J_i(\mathbf{r},t)$ in the bus bar (s. Sec. 4).

As described in [2] the two partial windings of the secondary side are modelled with a total of eight prismatic bodies according to Figure 1. An external current density

$$J_{\text{sec}}(t) = \frac{N i_2(t)}{A_{\text{sec}}} \quad (1)$$

with $i_2(t)$ denoting the secondary current calculated during the transient simulation and A_{sec} being the cross-sectional area of the secondary winding is fed into each of the eight subdomains of the secondary winding as an external current density with the respective direction and sign. Here, the electrical conductivity has been set to $\sigma = 10 \text{ S/m}$ in order to suppress eddy currents in the secondary winding, which is composed of thin wires, but modelled as bulk material. The electrical conductivity of the materials assigned to the domains of the primary and secondary windings is set to be linearly dependent on the temperature of the thermal model (s. Sec. 5).

In order to avoid circular variable definitions in constitutive relations [3], the non-linear magnetic behavior of the ferromagnetic transformer core is considered using the $\mathbf{H} = f(|\mathbf{B}|)\mathbf{e}_B$ form. Starting from a linear interpolation as described in [2], different approaches for modelling the magnetic characteristic were investigated, which are listed in Tab. 1. In general, measurement data are used in a look-up table for interpolating the HB-behavior of a material, or as a basis for defining a global approximation function. If the measurement data are used in a look-up table, one has to assure that the interpolation function

- includes the data point [0 T, 0 A/m] for reasons of numerical stability,
- is continuous in the whole parameter range, and
- shows an asymptotic behaviour in the range of complete saturation (differential relative permeability $\mu_{r \text{ diff}} \rightarrow 1$).

Monotony of the interpolation function has a remarkable influence on convergence and solution time (Tab. 1). Depending on the interpolation approach and the quality of the measurement data it can be difficult to ensure a monotonic behavior (Fig. 2). Alternatively, a global approximation function can be found based on a $\mu(|B|)$ form [4]:

$$\mu_r = \frac{\mu_i - 1 + C_a B_N}{1 + C_b B_N + B_N^n} + 1 \quad (2)$$

The parameters

$$\mu_i = \mu|_{B=0} \quad (3)$$

and

$$B_N = \left| \frac{B}{B|_{\mu_r = \mu_{\text{max}}}} \right| = \left| \frac{B}{B_m} \right| \quad (4)$$

have a physical meaning, C_a , C_b and n are free parameters which have to be found by regression analysis of measurement data. The derived $H(|B|)$ relation is:

$$H = \frac{1}{\mu_0} \cdot \frac{B}{\frac{\mu_i - 1 + C_a (B/B_m)}{1 + C_b (B/B_m) + (B/B_m)^n} + 1} \quad (5)$$

Eq. 2 rather models the behavior of the differential instead of the absolute material permeability. Therefore Eq. 5 is an approximation which is only valid for μ_r much larger than one.

Table 1. Interpolation approaches for nonlinear ferromagnetic materials

Approximation approach	Relative solution time
Piecewise cubic interpol.	1.0
Global rational function	1.3
Linear interpolation	4.0
Cubic spline interpolation	≈ 100
Nearest neighbour	no convergence

Figure 3 exemplarily depicts global approximation functions of several materials which were derived from measurement data by the Levenberg-Marquardt algorithm. The numerical behavior is similar to a piecewise cubic interpolation. However, the effort for finding the parameters of the global function is low as compared to that for preparing the measurement data for an interpolation approach.

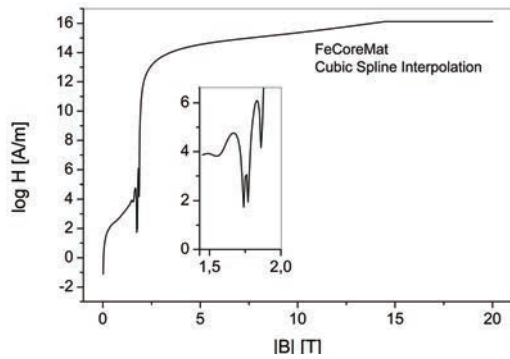


Figure 2. Non-monotonic curve $H = (|B|)$ obtained for a material “FeCoreMat” by using a cubic spline interpolation,

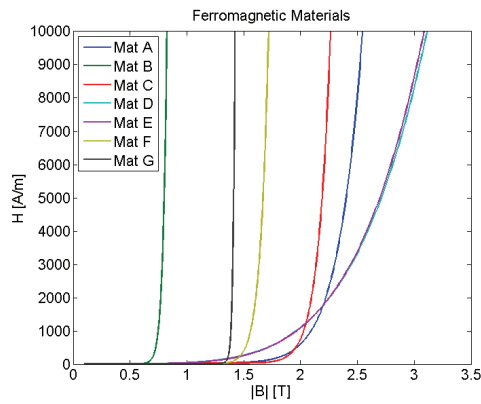


Figure 3. Magnetic field strength H versus flux density B of several simulated non-linear ferromagnetic materials based on Eq. (5)

Free meshing with user-controlled tetrahedral elements was applied with the predefined mesh size ‘normal’. The primary conductor and the core need a manually restricted maximum element size in order to simulate eddy currents and to ensure convergence.

The *mf* mode of the transformer model is coupled to other physics modes. A *cir* mode models the external circuitry on the primary and

secondary sides, a *ge* mode is used to couple the external primary current i_1 to the primary current density J_1 , two *dode* modes are used to compute spatially distributed time averages of the power loss density, and a *ht* mode is utilized to build the thermal model. Details are given in the following sections.

3. Coupling with SPICE Components

The FE model of the transformer is coupled to a sinusoidal current source at the primary side and to an external load resistor at the secondary side (Fig. 4). Both external circuits are modeled together in one *cir* mode. Different from the model presented in [2] we built the circuitry from the predefined components provided with the *cir* mode rather than importing it as a SPICE netlist.

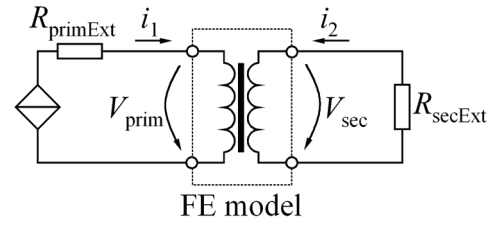


Figure 4. Primary and secondary circuits coupled to the FE model of the transformer

A sinusoidal 50 Hz current

$$i_1(t) = 1000 \text{ A} \cdot \sin(2\pi 50 \text{ s}^{-1} t) \quad (6)$$

is fed into the primary winding. The resistor $R_{\text{primExt}} = 1 \Omega$ is included for reasons of numerical stability.

At the secondary side, an external load resistor $R_{\text{secExt}} = 25 \Omega$ is connected to the winding terminals using an *External I vs. U* component coupled to the secondary voltage V_{sec} . V_{sec} is defined as a variable of the model:

$$V_{\text{sec}} = R_{\text{coil}} i_2 - V_i. \quad (7)$$

$R_{\text{coil}} = 25 \Omega$ denotes the internal coil resistance of the secondary winding within the FE model, and i_2 the secondary current through the external load resistor R_{secExt} . V_i is the voltage induced in the complete secondary winding:

$$V_i = \frac{N(V_1 + V_2 + \dots + V_8)}{A_{\text{sec}}}. \quad (8)$$

V_i is derived from the sum $V_1+V_2+\dots+V_8$ of the volume integral of the electric field strength in the direction of the current in each of the eight prismatic subdomains [2].

If eddy currents are suppressed, i. e. if the electrical conductivity of the primary conductor is set to a low value of e. g. 10 S/m, the external current density in the domain of the primary conductor J_{prim} can directly be deduced from i_1 and the current carrying cross section area A_{prim} of this conductor:

$$J_{\text{prim}} = i_1 / A_{\text{prim}} . \quad (9)$$

Otherwise, eddy currents will occur and the integral of the total current density over the cross sectional area of the conductor would be less than i_1 .

4. Modeling of Eddy Currents

The injection of a sinusoidal current with given amplitude and phase in the axial, here z -direction of the bus bar in the presence of eddy current effects in time-dependent simulations with COMSOL 4.2 is a bit tricky because only an external current density $J_{\text{ez}}(\mathbf{r}, t)$ can be applied to the domain representing the bus bar. However, a total primary current density $J_z(\mathbf{r}, t)$ over time has to be prescribed in the model. It is the sum of the external and the induced current density $J_{\text{iz}}(\mathbf{r}, t)$.

$$J_z(\mathbf{r}, t) = J_{\text{ez}}(\mathbf{r}, t) + J_{\text{iz}}(\mathbf{r}, t). \quad (10)$$

Straightforward allowance of eddy currents in the primary conductor by setting the electrical conductivity to that of copper would result in a total current density and thus in a current through the primary conductor that is smaller than the one supplied by the external current source. As a result, the simulated behaviour would be erroneous.

We used a global equation approach with a *ge* mode to ensure that the total primary current i_1 follows the predefined sinusoidal time course. A *ge* mode (Mathematics, ODE and DAE Interfaces, Global ODEs and DAEs) introduces an additional degree of freedom which determines the external current density J_{prim} inside of the domain of the primary conductor by the condition

$$i_1 - I_{\text{prim}} = 0 . \quad (11)$$

The total current I_{prim} in the primary conductor is not calculated only from an integration of J_{prim} but of the total current density J_z in the axial direction of the primary conductor (with length L_{prim}):

$$I_{\text{prim}} = \frac{1}{L_{\text{prim}}} \int_{(V_{\text{prim}})} J_z dV . \quad (12)$$

In this way, the model computes the space- and time-dependent eddy current density in the primary conductor (s. Fig. 5). This is important for a precise calculation of the current transmission accuracy and the losses of the non-ideal transformer during the simulation-based design.

However, this approach is not applicable to the secondary coil where eddy currents occur in each single turn. Here, a small conductivity value has still to be set in the respective domains.

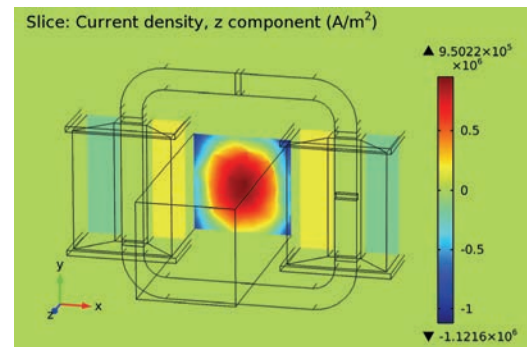


Figure 5. Simulated z -component of the total current density in the current carrying domains with skin effect in the primary conductor ($i_{1\text{peak}} = 1000$ A, $R_{\text{secExt}} = 20 \Omega$, $t = 0.23$ s)

5. Thermal Model

In general, electrical and magnetic material properties are temperature-dependent. Therefore, in a more detailed simulation of the behavior of current transformers the effects of self-heating should be considered. Therefore, we bi-directionally coupled the electromagnetic FE model to a thermal FE model of the assembly. Losses computed by the electromagnetic model are used to calculate the temperature field in the thermal model. The temperature field in turn determines the material properties in the electromagnetic model. Because of the periodicity of

the currents in the electromagnetic model the losses are also periodic with a stable mean value over one period under steady-state conditions. This allows coupling of the time-dependent electromagnetic model with a stationary thermal model when the time-dependent thermal behavior is not of interest.

The thermal model considers the following effects:

- heat sources, i. e. the primary and secondary conductor,
- heat conduction in solids and narrow air gaps,
- thermal contact resistances between solids which are in mechanical contact, e. g. between the coil bobbin and the coil,
- external convection and radiation at the outer surfaces of the solids.

As CFD simulations of the enclosing air would have been too time-consuming, heat exchange due to the external air convection was only taken into account in the form of Cauchy boundary conditions on the solid-air-interfaces. This approach is supported by the *ht* mode in COMSOL Multiphysics. Cauchy boundary conditions are characterized by specific heat convection coefficients which depend both on temperature and position. Normally, they are derived from empirical correlations [5]. This is already implemented in the *ht* mode. These correlations can not consider thermal interactions between solid-air-interfaces that are close to each other. Here, those interactions can be neglected, since the distance between most opposing solid-air-interfaces is larger than about two times the boundary layer thickness. In this case, contributions from convection become insignificant.

Radiation can be neglected as well at not too high temperatures.

The Ohmic losses are computed in the electromagnetic model. However, since the electric field is not solved for, the total power dissipation density *mf.Qh* which is implemented in COMSOL can not be used for the loss computation in our model. Instead, we applied two *dode* modes (Mathematics, ODE and DAE Interfaces, Domain ODEs and DAEs) for adding to the model an equation for the local heat density $Q(\mathbf{r}, t_i)$, which is generated by the local current density J :

$$Q(\mathbf{r}, t_i) = \int_0^{t_i} \frac{[J(\mathbf{r}, \tau)]^2}{\sigma} d\tau. \quad (13)$$

The time-average of the local loss power density in the time interval $[0, t_i]$ is

$$\bar{q}(\mathbf{r}, t_i) = \frac{Q(\mathbf{r}, t_i)}{t_i}. \quad (14)$$

This quantity is used as heat source field in the stationary thermal model. When the thermal model is solved for the first time before results of the time-dependent electromagnetic model are available, the $\bar{q}(\mathbf{r})|_{t_i=0}$ field is set to zero.

For the secondary winding (in which skin effect was suppressed by selecting a low conductivity value; s. Sec. 4) a correction factor has to be applied to the calculated heat density distribution in order to account for the actual conductivity.

6. Transient Electromagnetic-Thermal Simulation

In most applications the time scales of the electromagnetic and the thermal model are very different (e.g. ms versus min) if the thermal equilibrium is considered. Therefore we solved the problem by iterating alternate solutions of the two models. The solving sequence starts with a stationary study step of the thermal model with $q(\mathbf{r}) = 0$ as input and $T(\mathbf{r}) = T_{\text{amb}}$ as result. This homogeneous temperature field is used as input for the first time-dependent study step of the electromagnetic model. As a result after three (or more) simulated periods the time-averaged local power loss density $\bar{q}(\mathbf{r}, t^*)$ is obtained as a new input to the thermal model. In the next thermal simulation the new temperature field is then calculated and given back to the electromagnetic model, and so forth.

Solver settings for the stationary solver of the thermal model are not an issue, those for the time dependent solver of the electromagnetic model were set as follows:

- fully coupled, direct solver,
- linear system solver MUMPS,
- strict time stepping,
- time range 0.06 s (three 50 Hz periods).

Other settings remained at their default values. The thermal model inherits 66,290 DOF, the electromagnetic model 513,065 DOF. The simulations were done on an Intel i7 PC with 8 GB RAM running Windows Server 2008. The solu-

tion time was about 16 hours for a study including five stationary and four time-dependent study steps.

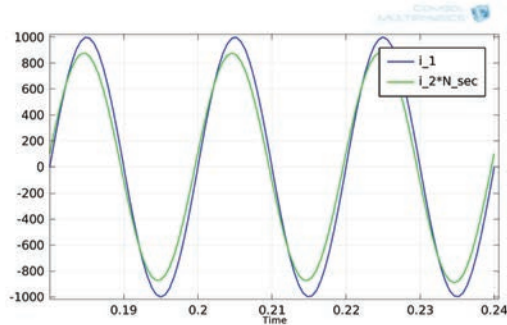


Figure 6. Simulated primary current i_1 and secondary current $i_2 \cdot N_2$ show an imperfect transformer coupling due to the air gaps in the core ($i_{1\text{peak}} = 1000 \text{ A}$, $R_{\text{secExt}} = 25 \Omega$)

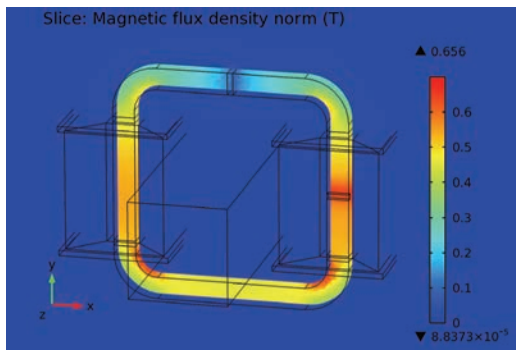


Figure 7. Simulated norm of the magnetic flux density in the center plane of the ferromagnetic transformer core ($i_{1\text{peak}} = 1000 \text{ A}$, $R_{\text{secExt}} = 20 \Omega$, $t = 0.23 \text{ s}$)

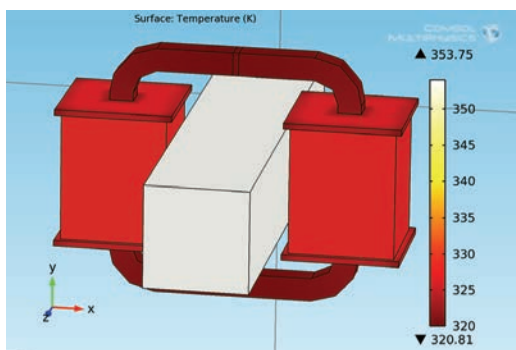


Figure 8. Simulated stationary temperature field at the surfaces of the solids ($i_{1\text{peak}} = 1000 \text{ A}$, $R_{\text{secExt}} = 20 \Omega$, $T_{\text{amb}} = 300 \text{ K}$)

The solutions usually converged within five iteration loops (Figure 9). Figure 6 depicts the simulated transient behaviour of the primary and

secondary currents for a typical example, Figure 7 the flux density distribution in the ferromagnetic transformer core, and Figure 8 the temperature distribution at the surfaces of the components. The model also simulates saturation effects in the transformer core and the current transmission error in the presence of air gaps.

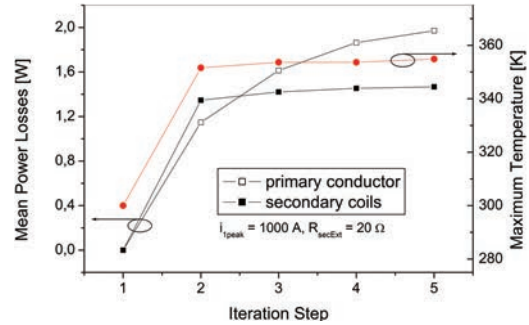


Figure 9. Mean power losses inside of the primary conductor and the secondary coils and maximum temperature as a function of the number of iterations

7. Summary and Outlook

The presented model allows transient FE analysis of transformers which are coupled to external circuitry. The transformer is modelled in the *mf* mode of COMSOL Multiphysics 4.2 which solves for the magnetic field. The non-linear magnetisation characteristic of the core material is accounted for in the form $\mathbf{H} = f(|\mathbf{B}|)\mathbf{e}_B$ based on a global rational approximation function. Transformer windings consisting of multiple turns are modeled as bulk regions. In the primary conductor, eddy currents are considered by means of a global equation. Because of their finer structure, skin effect can be neglected in the secondary windings. The electromagnetic model also computes the time-averaged power loss density distribution, which serves as an input for the thermal model. Vice versa, the temperature distribution computed by the thermal model is used as input to the electromagnetic model for controlling the temperature dependent electrical conductivity of the materials.

The thermal model takes both heat conduction in solids and external convection on surfaces by means of convection coefficients into account.

In particular, the developed model allows thorough analysis and design of the magnetic subsystem of transformers. This applies all the

more since the geometry is based on parametric modelling.

Future work will also focus on consideration of the transformer core lamination in the electromagnetic model, the anisotropic material behaviour inside of the coils.

References

1. G. Müller: *Elektrische Maschinen – Grundlagen, Aufbau und Wirkungsweise*, 7th ed., Verlag Technik, Berlin (1989)
2. T. Bödrich, H. Neubert, R. Disselnkötter: Transient Finite Element Analysis of a SPICE-coupled Transformer with COMSOL Multiphysics. 4th European COMSOL Conference, Paris (FR), 17.-19.11.2010
3. COMSOL AB: *Support Knowledge Base 852 – How can I model nonlinear magnetic materials?*, <http://www.comsol.com/support/knowledgebase/852/> (Sep. 10, 2010)
4. <https://modelica.org/libraries>
5. F.P. Incropera, D.P. DeWitt, T.L. Bergman, A.S. Lavine, *Fundamentals of Heat and Mass Transfer*, John Wiley and Sons, Hoboken (NJ), (2006)